PCCP

PAPER

View Article Online
View Journal | View Issue

Cite this: *Phys. Chem. Chem. Phys.*, 2021, **23**, 25152

Design and engineering of a dual-mode absorption/emission molecular switch for all-optical encryption†

Aaron D. Erlich, ‡ Nicholas P. Dogantzis, ‡ Lara Al Nubani, Lavinia A. Trifoi, Gregory K. Hodgson and Stefania Impellizzeri *

Received 20th August 2021,
Accepted 27th October 2021

DOI: 10.1039/d1cp03823k

rsc.li/pccp

Photochemical reactions that produce a detectable change in the spectroscopic properties of organic chromophores can be exploited to harness the principles of Boolean algebra and design molecule-based logic circuits. Moreover, the logic processing capabilities of these photoactive molecules can be directed to protect, encode, and conceal information at the molecular level. We have designed a photochemical strategy to read, write and encrypt data in the form of optical signals. We have synthesized a supramolecular system based on the known dye resazurin, and investigated a series of photochemical transformations that can be used to regulate its absorption and emission properties upon illumination with ultraviolet or visible light. We have then examined the logic behaviour of the photochemistry involved, and illustrated its potential application in data encryption.

Introduction

The development of molecular-scale information security and protection, encryption, and anticounterfeiting has sparked the interest of chemists since the first examples of functional molecular 'logic gates' were reported. The latter are molecules that can mimic Boolean logic operators and reproduce basic arithmetic functions.[1–7] Such systems are primarily based on organic molecular switches that can adjust their structural, electronic and spectroscopic properties when stimulated with chemical or photonic inputs and, in return, produce a detectable chemical, electrical or optical output that varies with the switching process.[8] Inputs and outputs can be encoded with binary digits (1 and 0), and the switching process devised to transduce a specific logic convention. Organic molecules can then be rationally designed and engineered to respond to specific combinations of physical, chemical, or biological signals, to generate a decision (True or 1; False or 0) according to the underlying logic operator, while their dimensions and synthetic 'bottom-up' accessibility offer practical access to ultraminiaturized building blocks with tailored structures and properties. Nonetheless, these switchable molecular systems can be also used in the context of information security, *i.e.* to implement data protection measures (at the molecular level) for their safer transport and communication.[9–14] Molecular security is currently achieved using cryptographic or steganographic methods to encrypt or hide a message.[15] For instance, invisible molecular 'inks' can be used to conceal text or images, securing the information from unauthorized copying;[16–24] similarly, erasable materials are valuable for storing sensitive or temporary data.[25–29] Stimuli-responsive chemical systems that deliver outputs in a nonlinear and not straightforward, predictable fashion are ideal candidates for both applications. To date, several examples of security inks have been reported using photochromic,[30–34] thermochromic,[22,34–37] electrochromic[38–41] and mechanochromic[42–44] compounds, all of which are able to communicate through changes in their absorption or emission properties. These changes are easily detected and quantified by spectroscopic analysis with high degrees of sensitivity and specificity. As such, these systems can be conveniently adapted to encode and conceal data, rather than processing it through logic operations.

These considerations prompted us to design a photochemical strategy to encode and encrypt data in the form of optical signals. Our approach relies on the photophysical and photochemical properties of switchable chromophores and the sequential regulation of their absorption signature upon illumination with ultraviolet or visible light.[45] Some of these chromophores also exhibit luminescence, which can be exploited as an

Department of Chemistry and Biology, Ryerson University, 350 Victoria Street, Toronto, Ontario, M5B 2K3, Canada. E-mail: simpellizzeri@ryerson.ca

† Electronic supplementary information (ESI) available: Evolution of the absorbance at 602 nm of **RZ** before and after irradiation at 525 nm; HPLC analysis of **RZ** before and after irradiation at 525 nm; absorption spectra of **RZ** before and after irradiation at 525 nm with 3 eq. NH_2OH; absorption and emission spectra of **2NB-RZ** before and after UVA irradiation; absorption spectra of **RZ** before and after irradiation at 365 nm with 3000 eq. NH_2OH; materials and methods; synthetic protocols; ^1H and ^{13}C NMR spectra. See DOI: 10.1039/d1cp03823k

‡ These authors contributed equally.

additional reading (output) channel. Compared to other strategies that are used to modulate the behavior of molecular switches (*e.g.*, addition of acids, bases or metal ions), light stimulation offers several advantages.[46,47] Besides the obvious lack of waste products, light can be delivered with high spatial and temporal resolution. Moreover, light does not require direct physical access, but can be operated remotely even on several individual logic elements at the same time – a considerable advantage for transferring the molecular logic systems from solution to the solid state. It follows that, in an all-photonic setup, barriers related to the concatenation of the logic devices are removed, as the inputs and outputs have physical equality. Under the relatively mild illumination conditions used, our systems display excellent photostability and fast response. Herein, we describe the design, synthesis and spectroscopic properties of these molecular-based switches, as well as the analysis of the basic Boolean functions that can be executed with them. Then, we demonstrate how their photoswitchable behaviour and the subsequent alteration of their spectroscopic profile can be harnessed for encrypting information expressed using a binary code, at the molecular level.

Results and discussion

Design and spectroscopy

All the compounds used in this work are illustrated in Scheme 1. The base chemical platform adopted is that of resazurin (**RZ** in Scheme 1). **RZ**, also known as Alamar Blue, is a phenoxazine-3-one dye frequently used for biological testing.[48,49] The absorption spectrum of a solution of **RZ** shows

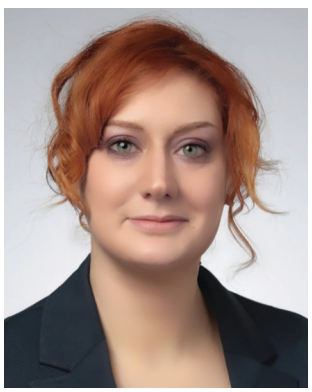

Stefania Impellizzeri

Stefania Impellizzeri is Assistant Professor in the Department of Chemistry and Biology of Ryerson University. She received a Laurea in Chemistry from the University of Bologna, a PhD in Chemistry from the University of Miami, and a Banting post-doctoral fellowship at the University of Ottawa. An expert in contemporary physical organic and materials chemistry, Professor Impellizzeri studies the discovery of new strategies to couple molecules and nanostructured materials, and original applications of single-molecule fluorescence microscopy techniques (tools that are traditionally employed in the biological sector) for the study of chemical phenomena, materials properties, chemical reactions, and catalysis. Her applied research is focused on the design and synthesis of switchable fluorescent probes for bioimaging, digital processing and communications with molecules (i.e., sensing and molecular computing), and nanoengineered textiles and coatings. She is member of the RSC, and the Board of Directors of Nano Ontario.

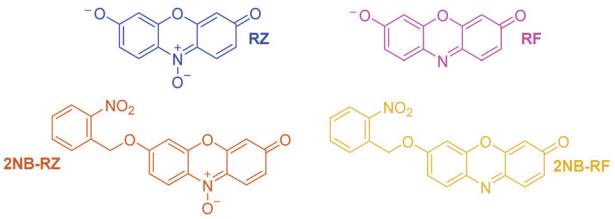

Scheme 1 Structures of compounds **RZ**, **RF**, **2NB-RZ** and **2NB-RF**.

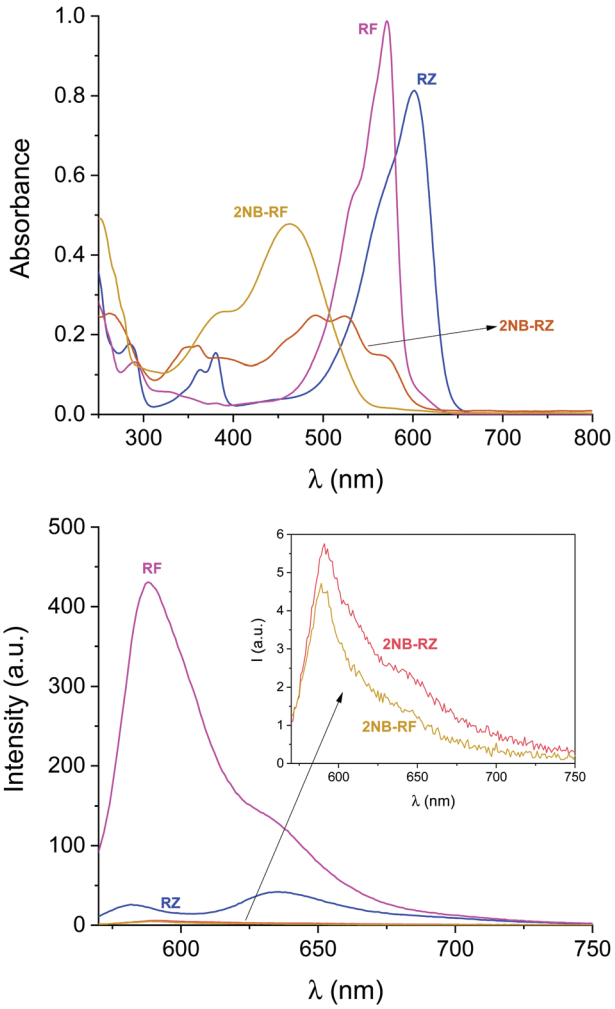

Fig. 1 Absorption (top panel) and emission (bottom panel, λ_{Ex} = 550 nm) spectra of **RZ**, **RF**, **2NB-RZ** and **2NB-RF** (18 μM). Spectra were recorded at 20 °C in H_2O (**RZ** and **RF**) or CH_3OH (**2NB-RZ** and **2NB-RF**) in the presence of NH_2OH (excess, 3000 eq.).

a band at λ_{Abs} = 602 nm (top panel in Fig. 1), which is responsible for its strong blue colouration. The spectrum also shows a weaker absorption at 380 nm. These bands are assigned to the π–π* transition of the phenoxazine-3-one and the n–π* transition of the N-oxide, respectively, as informed by previous investigations[50,51] and theoretical studies.[52] While **RZ** is weakly emissive (ϕ = 0.11), it can be irreversibly reduced to the strongly emissive resorufin (**RF** in Scheme 1, ϕ = 0.74).[50,51] This reaction, which is frequently observed in cellular,

enzymatic or microbiological assays, also causes the absorption to shift hypsochromically to λ_{Abs} = 573 nm and the solution to turn to a bright pink. The spectroscopic properties of **RZ** and **RF** can be altered by the chemical conjugation of a 2-nitrobenzyl (2NB) group to form **2NB-RZ** and **2NB-RF** (Scheme 1). **2NB-RZ** and **2NB-RF** were synthesized in one step by reacting **RZ** and **RF** with 2-nitrobenzyl bromide in the presence of base, to afford **2NB-RZ** and **2NB-RF** in 87% and 73% yields after purification (ESI†). The products were characterized by ^{1}H and ^{13}C NMR, FTIR and ESI-MS. Attachment of 2NB to **RZ** and **RF** affords two modified compounds that absorb between 490 and 600 nm (**2NB-RZ**, dark orange) and at 460 nm (**2NB-RF**, yellow), respectively. The blue shift of the absorption of the dyes is to be expected following either protonation or alkylation at the oxygen site, and the consequent change in bond length and geometry.[53] Critically, the coupling of nitrobenzyl groups to a dye's skeleton quenches the fluorescence of the chromophore.[54–57] In our case, this effect is particularly evident if we compare the emission spectra of resorufin **RF** and its 'caged' counterpart **2NB-RF** (bottom panel in Fig. 1). As resazurin **RZ** is already weakly fluorescent, the modification to **2NB-RZ** has lesser impact on the overall emission of the system; nevertheless, a decline in intensity is still observable, confirming the complete suppression of any residual luminescence (Fig. 1). All the spectra were recorded in the presence of excess hydroxylamine (NH_2OH) to maintain basic conditions. In fact, while the absorption of both **RZ** and **RF** are unaffected by pH changes in the range of 7.5–12, **RF** is highly fluorescent only at pH above 7.5.[50,51] Furthermore, the presence of the amine encourages the photochemistry at play (*vide infra*).

Photochemical switching of RZ to RF and fluorescence activation

The first component of our photochemical strategy to encrypt and encode data in the form of optical signals is the light-induced conversion of resazurin (**RZ**) to resorufin (**RF**) in the presence of hydroxylamine. **RZ** is stable under air in basic aqueous solution, however, UV-vis spectra of this same solution irradiated at 525 nm show the progressive disappearance of the typical **RZ** absorption at 602 nm and the concomitant appearance of the absorption of **RF** at 573 nm (top left panel in Fig. 2 and Fig. S1, ESI†) with an isosbestic point at 581 nm. The photochemical reaction proceeds as the solution turns from blue to pink. HPLC chromatograms recorded before and after irradiation confirm the formation of **RF** as the main product (Fig. S2, ESI†). The conversion process between **RZ** and **RF** relies on the photodeoxygenation of the N-oxide group, the deoxygenated product **RF** being the product formed. Previous reports have established that the mechanism involves, as a first step, electron transfer from the amine to the triplet excited state of **RZ**, leading to the formation of a charge transfer intermediate.[50,51,58] The presence of amines in sufficient concentration is required to ensure interaction with the triplet state of **RZ** and reduce the induction time.[59] Surely enough, the same experiment recorded using only 3 equivalents of NH_2OH leads to no

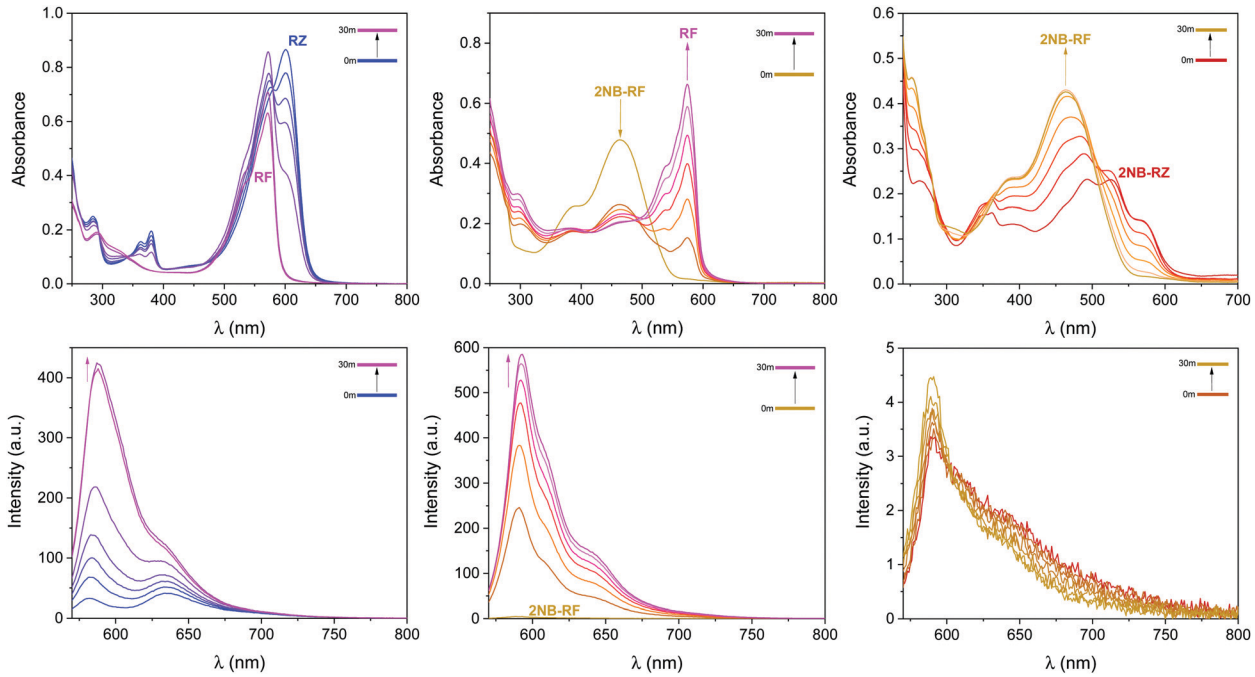

Fig. 2 General legend. Left column, **RZ**→**RF**. Center column, **2NB-RF**→**RF**; right column: **2NB-RZ**→**2NB-RF**. Absorption (top left panel) and emission (bottom left panel, λ_{Ex} = 550 nm) spectra of an aqueous solution of **RZ** (18 μM, 20 °C, NH_2OH 3000 eq.) before and after irradiation at 525 nm (0–30 min, 5 min irradiation intervals). Absorption (top center panel) and emission (bottom center panel, λ_{Ex} = 550 nm) spectra of a solution of **2NB-RF** (18 μM, 20 °C, CH_3OH, NH_2OH 3000 eq.) before and after irradiation at 365 nm (0–30 min, 5 min irradiation intervals). Absorption (top right panel) and emission (bottom right panel, λ_{Ex} = 550 nm) spectra of a solution of **2NB-RZ** (18 μM, 20 °C, CH_3OH, NH_2OH 3000 eq.) before and after irradiation at 525 nm (0–30 min, 5 min irradiation intervals).

observable change even after prolonged irradiation (Fig. S1 and S3, ESI†), consistent with comparable experiments reported using triethanolamine.[58] Interestingly, the presence of metal nanoparticles such as gold (AuNP) have been shown to reduce the induction time, and to be able to photocatalyze the conversion of **RZ** to **RF** using low concentrations of NH_2OH,[60–64] while higher temperatures can also favour the reaction.[64] As expected, the successful conversion of **RZ** into **RF** concurrently turns on the fluorescence (bottom left panel in Fig. 2). Thus, optical stimulation of this chemical system enables the generation and detection of an output, colour switching, in both absorption and emission modes. Indeed, the combination of these two modes within a single system could further extend the potential of these molecular switches to more sophisticated logic processors and encryption devices.

Photochemical switching of 2NB-RF to RF and fluorescence activation

The second component of our molecular-based encryption system is the photochemical conversion of **2NB-RF** into **RF**. These compounds incorporate the same chromophore, resorufin; however, **2NB-RF** comprises a photocleavable 2-nitrobenzyl group on the same covalent skeleton. Irradiation of 2-nitrobenzyl derivatives with ultraviolet light encourages the cleavage of the nitroaromatic group, freeing the parent species along with a nitrosocarbonyl product.[65] It follows that a solution of **2NB-RF** illuminated with UV light at 365 nm leads to the formation of **RF** and a concomitant bathochromic shift in absorption from 460 to 573 nm (top center panel in Fig. 2). An obvious colour change from yellow to pink is detectable with the naked eye. Based on the known molar extinction coefficient of **RF** in CH_3OH at 573 nm ($50\,000 \pm 2500\ M^{-1}\ cm^{-1}$),[50,51] we calculated that the final concentration of the product is $\sim$13 μM, corresponding to a 72% reaction yield. The emission spectrum of **2NB-RF** reveals a negligible change in emission wavelength with respect to the uncaged species, but a complete suppression of the fluorescence intensity. It is known that the fluorescence intensity of resorufin can easily be regulated by modification of its chemical structure. Specifically, protection of the 7-hydroxyl group weakens the intramolecular charge transfer (ICT) process, resulting in quenching. According to theoretical calculations,[52] resorufin exhibits strong hyperconjugative interactions ($n \rightarrow \sigma^*/\pi^*$) between all electron-donating oxygen atoms (two terminal and one bridge) and antibonding acceptors. Among the two terminal O atoms, the negatively charged O in 7-position (normally referred to as a ''hydroxylic oxygen'' as it can be subjected to protonation to form a hydroxy group) acts as the strongest electron-donating orbital. The ICT process depends on both donor and acceptor strength, as well as the extent of electronic coupling between the orbitals. However, covalent coordination of this oxygen prevents it to act as a donor (n) orbital, diminishing the ICT interaction from the electron-donating HOMO to the electron-acceptor LUMO and, thus, quenching the fluorescence emission. However, deprotection of the probe's substituent groups enables the recovery of the push–pull process and restores the emission.[66,67] In agreement with these considerations, the fluorescence of **2NB-RF** progressively increases under irradiation at 365 nm as the 2-nitrobenzyl quenching group is cleaved from the main chromophore structure, releasing the luminescent **RF** photoproduct (bottom center panel in Fig. 2).

Photochemical switching of 2NB-RZ to 2NB-RF

Next, we wondered if the photochemical conversion between resazurin and resorufin, induced by illumination of **RZ** with green light, could take place even with the protected substrate **2NB-RZ**. The relative absorption of **2NB-RZ** at the irradiation wavelength of 525 nm is $\sim$70% of that of an equimolar solution of **RZ** recorded under otherwise identical conditions (Fig. 1). As such, we sought to determine if **2NB-RZ** had the potential to undergo a photochemical pathway similar to its uncaged counterpart. Experiments were conducted in the presence of an excess of NH_2OH which, despite having no effect on the nitroarene substituent, is necessary to promote the photochemical transformation within the chromophore. The results of this experiment confirmed our hypothesis, and the conversion of the protected resazurin to protected resorufin is indeed possible. As shown in Fig. 2 (top right panel), the absorption of a CH_3OH solution of **2NB-RZ** exposed to visible light gradually blue shifts until a new maximum at 460 nm, characteristic of **2NB-RF**, is formed. Further, the shift is accompanied by the loss of the vibrational pattern of **2NB-RZ**. As can be seen from these spectroscopic changes, the reaction is quantitative after 30 minutes of irradiation. In the fluorescence channel (bottom right panel in Fig. 2), the emission intensity does not change with increasing irradiation time, confirming that the structural integrity of the 2-nitrobenzyl appendix is maintained under these excitation conditions. Thus, the photochemical behaviour of the caged resazurin can be preserved even in the presence of the protecting group.

Combinatorial photoswitching of 2NB-RZ

Inspired by these results, we investigated the ability of **2NB-RZ** to distinguish between consecutive input sequences (ultraviolet and visible illumination in alternating order). First, we investigated the outcome of the visible + ultraviolet consecutive optical stimulation string. This specific sequence of events is anticipated to yield the caged resorufin compound **2NB-RF** upon illumination with green light, followed by the UV-induced photocleavage of the 2-nitrobenzyl moiety to yield free **RF**. The complete photochemical reaction pathway is **2NB-RZ**→**2NB-RF**→**RF**. The reaction can be monitored through colorimetric changes in both the absorption and the fluorescence channels. The overall transformation was verified by the emergence of a band at λ_{Abs} = 460 nm (**2NB-RF**) during the visible illumination cycle, followed by a bathochromic shift to λ_{Abs} = 573 nm (**RF**) as the light source is switched to 365 nm. In emission mode, this progression of events should also be accompanied by fluorescence 'turn on' only after execution of the second input command (UVA). To our delight, the absorption spectra of a CH_3OH solution of **2NB-RZ** recorded before light irradiation (a in Fig. 3A), after irradiation at 525 nm (b in Fig. 3A), and after the consecutive

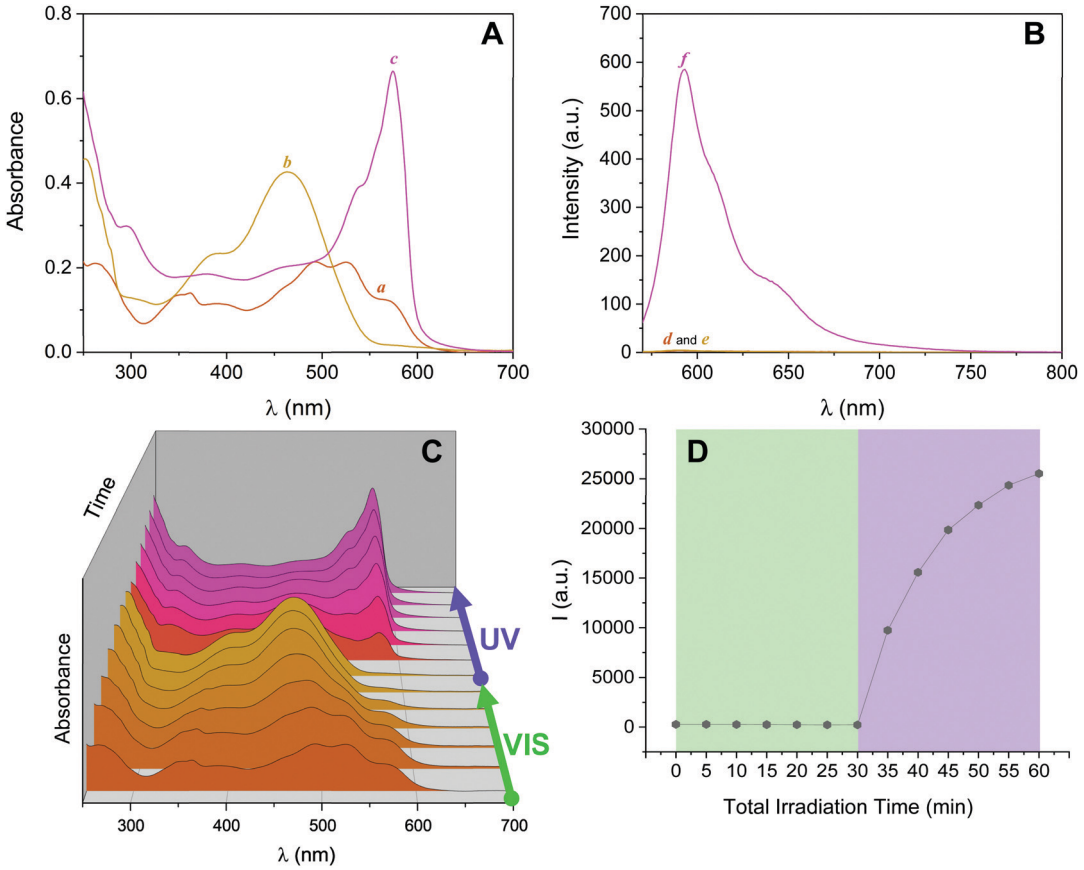

Fig. 3 Top panels: Absorption (panel A) and emission (panel B, λ_{Ex} = 550 nm) spectra of a solution of **2NB-RZ** (18 μM, 20 °C, CH_3OH, NH_2OH 3000 eq.) before irradiation (a and d), after irradiation at 525 nm (b and e, 30 min) and after additional irradiation at 365 nm (c and f, 30 min). Bottom panels: Evolution of the absorbance (panel C) and integrated emission intensity (panel D) during the illumination cycles.

525/365 nm optical stimulation (c in Fig. 3A) prove that this is the case. In parallel, the fluorescence pattern shows no change in intensity during the first irradiation cycle as the 2-nitrobenzyl quencher is unaffected by the transformation of the parent resazurin to resorufin (d and e in Fig. 3B), but it experiences a sudden increase in intensity as the photocage is removed with ultraviolet light (f in Fig. 3B). A comparison between the temporal evolution of the integrated emission intensity under irradiation at 525 nm *versus* the same solution exposed to 365 nm light over the same period of time (Fig. 3D) confirms that ultraviolet illumination is essential to activate fluorescence. Therefore, this protocol allows the regulation of the relative amounts of the three participating species, and hence the spectroscopic signature (Fig. 3C) and the emission intensities (Fig. 3D) detected at a given time, simply by controlling the optical source and the irradiation time.

We attempted to operate the multiresponsive chemical system **2NB-RZ** using the same combination of optical stimuli, UV and visible light, in inverse order. That is, **2NB-RZ** was targeted by illumination at 365 nm, followed by exposure to 525 nm radiation. This string of events should, in principle, generate an alternate set of participating molecular species following the reaction pathway **2NB-RZ**→**RZ**→**RF**, ultimately achieving the same final state and output (strong absorption at 573 nm and high fluorescence) but following a reverse route. We hence sought to explore if **2NB-RZ** could differentiate between the two different input sequences and lead to an identical final chemical state (**RF**) by following a parallel circuitry. Remarkably however, ultraviolet irradiation of **2NB-RZ** actually yields **RF** in one step. The direct photochemical transformation can be monitored by both absorption (Fig. 4, top panel) and emission (Fig. 4, bottom panel) spectroscopy. On scale, original spectra are shown in Fig. S4 (ESI†). A control experiment performed by irradiating a solution of **RZ** at 365 nm revealed that the UVA-induced photoconversion to **RF** in aqueous basic conditions is completely ineffective in the absence of the 2-nitrobenzyl appendage (Fig. S5, ESI†). Evidently, the two processes (uncaging and **RZ**→**RF**) occur simultaneously and the final state **RF** is reached *via* an alternative pathway. The photochemical, UV-induced deoxygenation of N-oxides is in fact a known process, with systems carrying electron-withdrawing substituents applying a stabilizing effect on the excited state and thereby favouring photoreduction.[48] It follows that conjugation of resazurin to the nitroarene likely enables selective access to the n–π* state of the N-oxide and, as a consequence, direct localization of the excitation energy on the dissociating N–O bond.

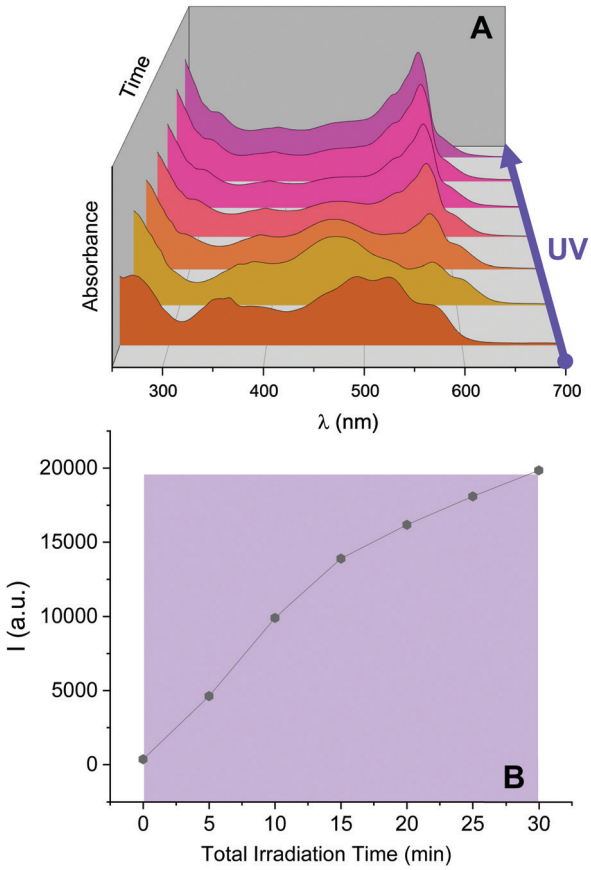

Fig. 4 Evolution of the absorbance (top panel) and integrated emission intensity (bottom panel, λ_{Ex} = 550 nm) of a solution of **2NB-RZ** (18 μM, 20 °C, CH_3OH, NH_2OH 3000 eq.) before and after irradiation at 365 nm (0–30 min, 5 min irradiation intervals).

Elementary logic and code encryption applications

The multistate molecular switch **2NB-RZ** detects two optical signals. They are ($\mathbf{I_1}$) ultraviolet light and ($\mathbf{I_2}$) visible light. In the presence of base, it responds to these stimulations by generating two output signals, which are ($\mathbf{O_1}$) the absorption band of **2NB-RF** at 460 nm and ($\mathbf{O_2}$) the absorption of **RF** at 573 nm. Each input signal can be either on or off and can be represented using binary digits, *i.e.*, it can assume only the two values 1 (high) or 0 (low). In other words, this molecular system can read a string of two binary inputs and write a specific combination of binary outputs. For example, when both $\mathbf{I_1}$ and $\mathbf{I_2}$ stimulations are off – and the input string is 00 – the molecular switch is in the state **2NB-RZ** which does not have strong absorption at either 460 or 573 nm (Fig. 1). As a result, the two output signals $\mathbf{O_1}$ and $\mathbf{O_2}$ are low, and the output string is 00. Instead, if $\mathbf{I_1}$ is off while $\mathbf{I_2}$ is on, the input string is 01. Under these conditions (green light), the molecular switch is in state **2NB-RF**, which has a strong absorption at 460 nm only. In such case, the output $\mathbf{O_1}$ is high while $\mathbf{O_2}$ is low. All the possible combinations of input data and the corresponding output results are summarized in Table 1. Note that another output channel, $\mathbf{O_3}$, can be added to the truth table by switching the analysis mode to the fluorescence channel. In fact, of all the interconvertible systems illustrated in Scheme 1, only one (**RF**) is fluorescent (λ_{Em} = 592 nm). While the logic transduction of $\mathbf{O_3}$ mirrors that of $\mathbf{O_2}$ (Table 1), as they both correspond to the same chemical state, they can be exploited independently for encryption purposes since they are 'read' differently (excitation is required to visualize fluorescence). From Table 1, it can be deduced that the logic behaviour of the molecular switch **2NB-RZ** corresponds to that of INH ('inhibit') and YES ('buffer') logic gates (Scheme 2). The buffer gate does not change the logic relationship between the input and output, but functions as an amplifier for an input signal to achieve increased output expression capability for downstream connected logic components.

Finally, it is important to notice that all the output signals we described are detectable in the presence of NH_2OH, which is essential to promote the various photochemical conversions. As such, the presence of base cannot be considered an input stimulation *per se*, and for the logic purposes alone its role is similar to that of the solvent. Nevertheless, recall that the spectroscopic properties of **RZ** and **RF** are pH dependent, and that their absorption and emission signatures can be dramatically altered upon acidification of the solution. Although the utilization of chemical stimulations (such as acid or base) is not part of this work, which focuses solely on optical inputs to switch the spectroscopic response of our systems, it is reasonable to suggest that the truth table below could be further expanded with an additional input column, $\mathbf{I_3}$, representing acid.

Through the photochemical conversions that are possible between the molecular components shown in Scheme 1, different colorimetric states can be obtained. Scheme 3 summarizes the conditions by which the spectroscopic response can be controlled,

Table 1 Truth table of the molecular switch **2NB-RZ**. The two inputs $\mathbf{I_1}$ and $\mathbf{I_2}$ are ultraviolet (365 nm) and visible (525 nm) light irradiation, respectively. Output $\mathbf{O_1}$ is absorption at 460 nm, and output $\mathbf{O_2}$ is absorption at 573 nm. Output $\mathbf{O_3}$ is fluorescence (λ_{Em} = 592 nm)

$\mathbf{I_1}$ (UVA)	$\mathbf{I_2}$ (VIS)	$\mathbf{O_1}$ (A@460 nm)	$\mathbf{O_2}$ (A@573 nm)	$\mathbf{O_3}$ (fluorescence)
Off	Off	Low	Low	Low
Off	On	High	Low	Low
On	Off	Low	High	High
On	On	Low	High	High

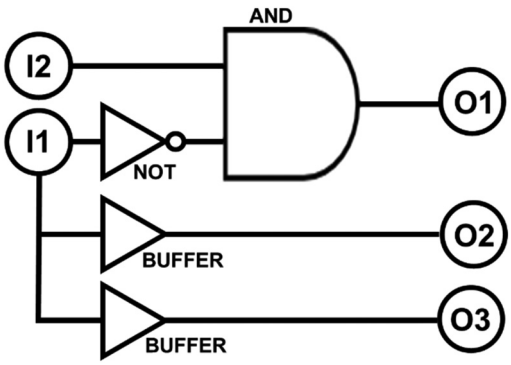

Scheme 2 The logic circuit representative of the behaviour of the molecular switch **2NB-RZ**.

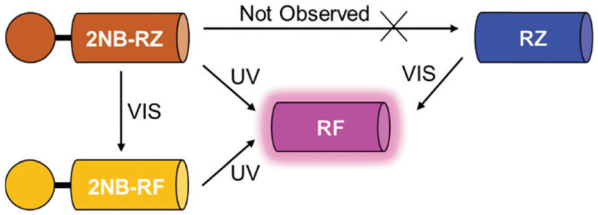

Scheme 3 All the possible photochemical conversions of compounds **RZ**, **2NB-RZ**, and **2NB-RF**.

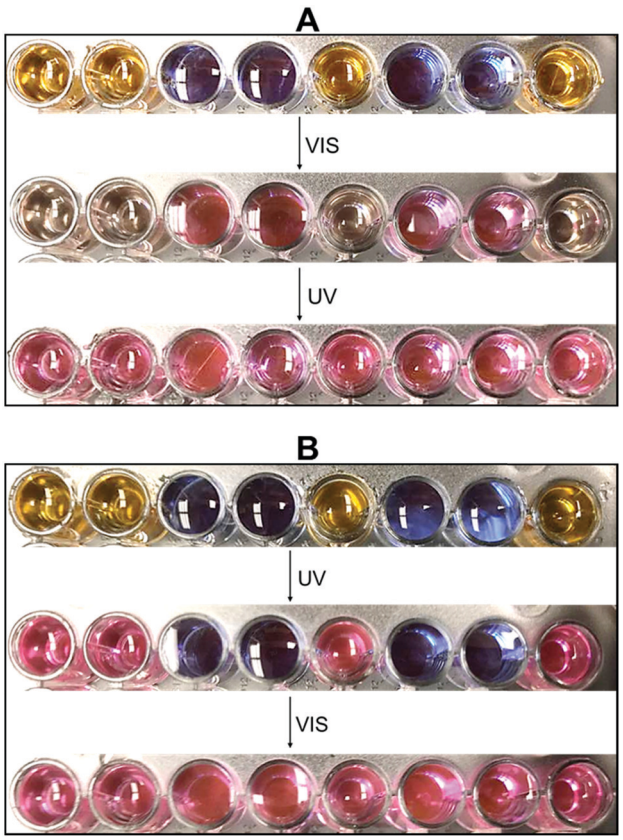

Fig. 5 Binary models for applying **2NB-RZ** (dark yellow plates) and **RZ** (blue plates) in information encryption using UV (365 nm) and VIS (525 nm) as password entries.

and the Boolean network established. The glowing structure in Scheme 3 represents a fluorescent species.

Based on the multidimensional spectrometric behaviour illustrated in Scheme 3, we demonstrated the encryption ability of our systems by loading a binary code in standard 8 bit ASCII characters. For proof-of-concept, we selected a combination of **2NB-RZ** and **RZ** and arranged them in a defined order using a well plate. These solutions, stored in the dark under air, did not show any noticeable change in colour to the naked eye up to 72 h. We can then choose the full message to be read using output $\mathbf{O_2}$ – absorption at 573 nm, corresponding to a bright pink colour under natural light – as the decryption key. As shown in Fig. 5A, both the input illumination sequences, VIS and UV, are required to visualize all bits of information. The same result can be attained, using the very same combination and order of starting materials, by inverting the chain of inputs, UV and then VIS (Fig. 5B). Nonetheless, notice how operating only one of the inputs (UV or VIS) enables the decryption of only some sections (bits) of the sequence. Hence, sensitive information can be hidden in smaller subsets of a larger series of characters/sentences for double encryption purposes, where the two optical inputs are used distinctively as password entries that unlock only specific parts of the code. This requirement of using two independent activations sources is similar to the concept of two-factor authentication. If an excitation source is available, the detection mode can be switched from absorption to fluorescence, where the quenched and strong red fluorescence spots represent the states of 0 (low) and 1 (high), respectively (Table 1).

Conclusions

We conducted a quantitative photophysical investigation of the known organic dyes resazurin and resorufin, along with two photocaged derivatives. The latter are based upon the covalent conjugation between the resazurin and resorufin chromophores and a 2-nitrobenzyl unit, and were synthesized in one step. Further, we probed the photochemical behaviour of the four species under ultraviolet (365 nm) and visible (525 nm) illumination. Specifically, we studied the visible light-induced photoreduction of resazurin in the presence of hydroxylamine using either the 'naked' chromophore or its caged counterpart, which produces resorufin or 2-nitrobenzyl resorufin depending on the choice of substrate. We then examined the photochemical behaviour of caged resorufin and caged resazurin under UV light. Interestingly, while in the first case we observed photocleavage of the 2-nitrobenzyl group to yield resorufin, the irradiation of 2-nitrobenzyl resazurin leads to the direct formation of resorufin. In contrast, the deoxygenation of resazurin to resorufin is inhibited under UV light in the absence of the nitroarene appendix. These results highlight how the photochemistry of resazurin can be modulated through the strategic modification of its chemical structure. The four dyes all possess a unique absorption signature that can be used to distinguish between them, and can thus be exploited to encode binary digits into optical outputs. 2-Nitrobenzyl resazurin in particular, can respond to two optical inputs and produce three optical outputs (two in absorption mode, one in fluorescence mode) resulting from the transformation into either resorufin or 2-nitrobenzyl resorufin encouraged by UV and visible illumination, respectively. Overall, this chromophore can transduce the 'inhibit' and 'buffer' (amplifier) logic operators into a single unimolecular system. The fast photochemical response of the various molecular components can be applied to information encryption and protection, and a proof-of-concept encoding protocol has been demonstrated.

Conflicts of interest

The authors declare no competing financial interests.

Acknowledgements

We thank the Natural Sciences and Engineering Research Council of Canada (Discovery Grant) and Ryerson University. This research has also been supported by the Ryerson University Faculty of Science Dean's Research Fund. N. P. Dogantzis acknowledges the receipt of a Ryerson University Graduate Scholarship and an Ontario Graduate Scholarship. L. Al Nubani acknowledges the receipt of a Ryerson Undergraduate Research Opportunity (URO). We thank Robert Denning for support with chromatographic data.

References

1 A. P. de Silva, *Molecular Logic-based Computation*, Royal Society of Chemistry, Cambridge, 2012.
2 A. P. de Silva, *Molecular and Supramolecular Information Processing*, Wiley-VCH Verlag GmbH & Co. KGaA, Weinheim, Germany, 2012.
3 A. P. de Silva and S. Uchiyama, Molecular logic and computing, *Nat. Nanotechnol.*, 2007, **2**, 399.
4 F. M. Raymo, Digital processing and communication with molecular switches, *Adv. Mater.*, 2002, **14**, 401–414.
5 S. Erbas-Cakmak, S. Kolemen, A. C. Sedgwick, T. Gunnlaugsson, T. D. James, J. Yoon and E. U. Akkaya, Molecular logic gates: the past, present and future, *Chem. Soc. Rev.*, 2018, **47**, 2228–2248.
6 K. Szaciłowski, *Infochemistry*, John Wiley & Sons, Ltd, Chichester, UK, 2012.
7 K. Szaciłowski, Digital Information Processing in Molecular Systems, *Chem. Rev.*, 2008, **108**, 3481–3548.
8 B. L. Feringa and W. R. Browne, *Molecular Switches*, Wiley-VCH Verlag GmbH & Co. KGaA, Weinheim, Germany, 2011.
9 B. Finkler, I. Riemann, M. Vester, A. Grüter, F. Stracke and G. Jung, Monomolecular pyrenol-derivatives as multi-emissive probes for orthogonal reactivities, *Photochem. Photobiol. Sci.*, 2016, **15**, 1544–1557.
10 T. Sarkar, K. Selvakumar, L. Motiei and D. Margulies, Message in a molecule, *Nat. Commun.*, 2016, **7**, 11374.
11 A. C. Boukis, K. Reiter, M. Frölich, D. Hofheinz and M. A. R. Meier, Multicomponent reactions provide key molecules for secret communication, *Nat. Commun.*, 2018, **9**, 1439.
12 O. Lustgarten, L. Motiei and D. Margulies, User Authorization at the Molecular Scale, *ChemPhysChem*, 2017, **18**, 1678–1687.
13 J. Andréasson and U. Pischel, Molecules for security measures: From keypad locks to advanced communication protocols, *Chem. Soc. Rev.*, 2018, **47**, 2266–2279.
14 J. O. Holloway, F. Van Lijsebetten, N. Badi, H. A. Houck and F. E. Du Prez, From Sequence-Defined Macromolecules to Macromolecular Pin Codes, *Adv. Sci.*, 2020, **7**, 1903698.
15 B. Schneier, *Secrets and Lies*, Wiley Publishing, Inc., Indianapolis, Indiana, 2015.
16 N. Zerby, O. Malka, S. Bhattacharya, N. Nandha Kadamannil, M. Baranov and R. Jelinek, Crystallization-Induced Emissive Invisible Ink, *Adv. Opt. Mater.*, 2019, **7**, 1900232.
17 Z. Xu, D. Gonzalez-Abradelo, J. Li, C. A. Strassert, B. J. Ravoo and D.-S. Guo, Supramolecular color-tunable photoluminescent materials based on a chromophore cascade as security inks with dual encryption, *Mater. Chem. Front.*, 2017, **1**, 1847–1852.
18 Y.-M. Wang, X.-T. Tian, H. Zhang, Z.-R. Yang and X.-B. Yin, Anticounterfeiting Quick Response Code with Emission Color of Invisible Metal–Organic Frameworks as Encoding Information, *ACS Appl. Mater. Interfaces*, 2018, **10**, 22445–22452.
19 S. L. Sonawane and S. K. Asha, Fluorescent Polystyrene Microbeads as Invisible Security Ink and Optical Vapor Sensor for 4-Nitrotoluene, *ACS Appl. Mater. Interfaces*, 2016, **8**, 10590–10599.
20 T. K. Mondal and S. K. Saha, Facile Approach To Synthesize Nitrogen- and Oxygen-Rich Carbon Quantum Dots for pH Sensor, Fluorescent Indicator, and Invisible Ink Applications, *ACS Sustainable Chem. Eng.*, 2019, **7**, 19669–19678.
21 Y. Liu, L. Zhou, Y. Li, R. Deng and H. Zhang, Highly fluorescent nitrogen-doped carbon dots with excellent thermal and photo stability applied as invisible ink for loading important information and anti-counterfeiting, *Nanoscale*, 2017, **9**, 491–496.
22 A. Khatami, S. S. Prova, A. K. Bagga, M. Yan Chi Ting, G. Brar and D. R. Ifa, Detection and imaging of thermochromic ink compounds in erasable pens using desorption electrospray ionization mass spectrometry, *Rapid Commun. Mass Spectrom.*, 2017, **31**, 983–990.
23 A. Kalita, A. H. Malik and N. Sen, Sarma, Stimuli-Responsive Naphthalene Diimide as Invisible Ink: A Rewritable Fluorescent Platform for Anti-Counterfeiting, *Chem. – Asian J.*, 2020, **15**, 1074–1080.
24 Y. Gu, C. He, F. Liu and J. Ye, Raman Ink for Steganography, *Adv. Opt. Mater.*, 2021, **9**, 2002038.
25 P.-H. Wang, C.-M. Yu, M.-S. Wang and G.-C. Guo, Viologen-based photochromic coordination compounds for inkless and erasable prints, *Dyes Pigm.*, 2021, **185**, 108888.
26 J. Wang, B. Jin, N. Wang, T. Peng, X. Li, Y. Luo and S. Wang, Organoboron-Based Photochromic Copolymers for Erasable Writing and Patterning, *Macromolecules*, 2017, **50**, 4629–4638.
27 Q. Shi, S.-Y. Wu, X.-T. Qiu, Y.-Q. Sun and S.-T. Zheng, Three viologen-derived Zn-organic materials: photochromism, photomodulated fluorescence, and inkless and erasable prints, *Dalton Trans.*, 2019, **48**, 954–963.
28 A. Kishimura, T. Yamashita, K. Yamaguchi and T. Aida, Rewritable phosphorescent paper by the control of competing kinetic and thermodynamic self-assembling events, *Nat. Mater.*, 2005, **4**, 546–549.
29 H. Jin, H. Li, Z. Zhu, J. Huang, Y. Xiao and Y. Yan, Hydration-Facilitated Fine-Tuning of the AIE Amphiphile Color and Application as Erasable Materials with Hot/Cold Dual Writing Modes, *Angew. Chem., Int. Ed.*, 2020, **59**, 10081–10086.
30 Y. Yang, L. Guan, H. Jiang, L. Duan and G. Gao, A rapidly responsive photochromic hydrogel with high mechanical strength for ink-free printing, *J. Mater. Chem. C*, 2018, **6**, 7619–7625.
31 S. Seipel, J. Yu, A. P. Periyasamy, M. Viková, M. Vik and V. A. Nierstrasz, Inkjet printing and UV-LED curing of photochromic dyes for functional and smart textile applications, *RSC Adv.*, 2018, **8**, 28395–28404.

32 T. V. Pinto, P. Costa, C. M. Sousa, C. A. D. Sousa, C. Pereira, C. J. S. M. Silva, M. F. R. Pereira, P. J. Coelho and C. Freire, Screen-Printed Photochromic Textiles through New Inks Based on SiO2@naphthopyran Nanoparticles, *ACS Appl. Mater. Interfaces*, 2016, **8**, 28935–28945.
33 R. Klajn, P. J. Wesson, K. J. M. Bishop and B. A. Grzybowski, Writing Self-Erasing Images using Metastable Nanoparticle ''Inks'', *Angew. Chem., Int. Ed.*, 2009, **48**, 7035–7039.
34 M. Avella-Oliver, S. Morais, R. Puchades and Á. Maquieira, Towards photochromic and thermochromic biosensing, *TrAC, Trends Anal. Chem.*, 2016, **79**, 37–45.
35 M. Vukoje, S. Miljanić, J. Hrenović and M. Rožić, Thermochromic ink–paper interactions and their role in biodegradation of UV curable prints, *Cellulose*, 2018, **25**, 6121–6138.
36 R. Kulčar, M. Friškovec, N. Hauptman, A. Vesel and M. K. Gunde, Colorimetric properties of reversible thermochromic printing inks, *Dyes Pigm.*, 2010, **86**, 271–277.
37 S. Cho, G. Kim, S. Lee, J. Park and W. Shim, Molecular-Printed Thermochromic with Fast Color Switching, *Adv. Opt. Mater.*, 2017, **5**, 1700627.
38 J. M. Wang, X. W. Sun and Z. Jiao, Application of Nanostructures in Electrochromic Materials and Devices: Recent Progress, *Materials*, 2010, **3**, 5029–5053.
39 A. M. Österholm, D. E. Shen, D. S. Gottfried and J. R. Reynolds, Full Color Control and High-Resolution Patterning from Inkjet Printable Cyan/Magenta/Yellow Colored-to-Colorless Electrochromic Polymer Inks, *Adv. Mater. Technol.*, 2016, **1**, 1600063.
40 M. Möller, S. Asaftei, D. Corr, M. Ryan and L. Walder, Switchable Electrochromic Images Based on a Combined Top–Down Bottom–Up Approach, *Adv. Mater.*, 2004, **16**, 1558–1562.
41 H. Li, J. Chen, M. Cui, G. Cai, A. L.-S. Eh, P. S. Lee, H. Wang, Q. Zhang and Y. Li, Spray coated ultrathin films from aqueous tungsten molybdenum oxide nanoparticle ink for high contrast electrochromic applications, *J. Mater. Chem. C*, 2016, **4**, 33–38.
42 J. Sun, J. Han, Y. Liu, Y. Duan, T. Han and J. Yuan, Mechanochromic luminogen with aggregation-induced emission: implications for ink-free rewritable paper with high fatigue resistance and low toxicity, *J. Mater. Chem. C*, 2016, **4**, 8276–8283.
43 J. Chen, L. Xu, M. Yang, X. Chen, X. Chen and W. Hong, Highly Stretchable Photonic Crystal Hydrogels for a Sensitive Mechanochromic Sensor and Direct Ink Writing, *Chem. Mater.*, 2019, **31**, 8918–8926.
44 G. H. Lee, S. H. Han, J. Bin Kim, J. H. Kim, J. M. Lee and S.-H. Kim, Colloidal Photonic Inks for Mechanochromic Films and Patterns with Structural Colors of High Saturation, *Chem. Mater.*, 2019, **31**, 8154–8162.
45 X. Huang and T. Li, Recent progress in the development of molecular-scale electronics based on photoswitchable molecules, *J. Mater. Chem. C*, 2020, **8**, 821–848.
46 D. Gust, T. A. Moore and A. L. Moore, Molecular switches controlled by light, *Chem. Commun.*, 2006, 1169–1178.
47 J. Andréasson, U. Pischel, S. D. Straight, T. A. Moore, A. L. Moore and D. Gust, All-Photonic Multifunctional Molecular Logic Device, *J. Am. Chem. Soc.*, 2011, **133**, 11641–11648.
48 S. N. Rampersad, Multiple Applications of Alamar Blue as an Indicator of Metabolic Function and Cellular Health in Cell Viability Bioassays, *Sensors*, 2012, **12**, 12347–12360.
49 J. O'Brien, I. Wilson, T. Orton and F. Pognan, Investigation of the Alamar Blue (resazurin) fluorescent dye for the assessment of mammalian cell cytotoxicity, *Eur. J. Biochem.*, 2000, **267**, 5421–5426.
50 C. Bueno, M. L. Villegas, S. G. Bertolotti, C. M. Previtali, M. G. Neumann and M. V. Encinas, The Excited-State Interaction of Resazurin and Resorufin with Amines in Aqueous Solutions, *Photochem. Photobiol.*, 2002, **76**, 385–390.
51 H. A. Montejano, M. Gervaldo and S. G. Bertolotti, The excited-states quenching of resazurin and resorufin by p-benzoquinones in polar solvents, *Dyes Pigm.*, 2005, **64**, 117–124.
52 M. J. Kariyottu Kuniyil and R. Padmanaban, Theoretical insights into the structural, photophysical and nonlinear optical properties of phenoxazin-3-one dyes, *New J. Chem.*, 2019, **43**, 13616–13629.
53 D. Brühwiler, N. Gfeller and G. Calzaferri, Resorufin in the channels of zeolite L, *J. Phys. Chem. B*, 1998, **102**, 2923–2929.
54 F. M. Raymo, Photoactivatable synthetic fluorophores, *Phys. Chem. Chem. Phys.*, 2013, **15**, 14840–14850.
55 D. Puliti, D. Warther, C. Orange, A. Specht and M. Goeldner, Small photoactivatable molecules for controlled fluorescence activation in living cells, *Bioorg. Med. Chem.*, 2011, **19**, 1023–1029.
56 W. Li and G. Zheng, Photoactivatable fluorophores and techniques for biological imaging applications, *Photochem. Photobiol. Sci.*, 2012, **11**, 460–471.
57 F. M. Raymo, Photoactivatable synthetic dyes for fluorescence imaging at the nanoscale, *J. Phys. Chem. Lett.*, 2012, **3**, 2379–2385.
58 G. V. Porcal, M. S. Altamirano, S. G. Bertolotti and C. M. Previtali, Organized media effect on the photochemical deoxygenation of resazurin in the presence of triethanolamine, *J. Photochem. Photobiol., A*, 2011, **219**, 62–66.
59 K. G. G. C. De Silva, M. I. Ranasinghe and S. Chowdhury, Understanding the induction time associated with the photoredution of resazurin by hydroxylamine in the presence of gold nanoparticles as a photocatalyst, *React. Kinet., Mech. Catal.*, 2020, **131**, 965–977.
60 W. Xu, J. S. Kong, Y.-T. E. Yeh and P. Chen, Single-molecule nanocatalysis reveals heterogeneous reaction pathways and catalytic dynamics, *Nat. Mater.*, 2008, **7**, 992.
61 X. Zhou, W. Xu, G. Liu, D. Panda and P. Chen, Size-Dependent Catalytic Activity and Dynamics of Gold Nanoparticles at the Single-Molecule Level, *J. Am. Chem. Soc.*, 2010, **132**, 138–146.
62 P. Chen, W. Xu, X. Zhou, D. Panda and A. Kalininskiy, Single-nanoparticle catalysis at single-turnover resolution, *Chem. Phys. Lett.*, 2009, **470**, 151–157.
63 W. Xu, J. S. Kong and P. Chen, Probing the catalytic activity and heterogeneity of Au-nanoparticles at the single-molecule level, *Phys. Chem. Chem. Phys.*, 2009, **11**, 2767–2778.
64 C. J. B. Alejo, C. Fasciani, M. Grenier, J. C. Netto-Ferreira and J. C. Scaiano, Reduction of resazurin to resorufin

catalyzed by gold nanoparticles: dramatic reaction acceleration by laser or LED plasmon excitation, *Catal. Sci. Technol.*, 2011, **1**, 1506–1511.

65 P. Klán, T. Šolomek, C. G. Bochet, A. Blanc, R. Givens, M. Rubina, V. Popik, A. Kostikov and J. Wirz, Photoremovable Protecting Groups in Chemistry and Biology: Reaction Mechanisms and Efficacy, *Chem. Rev.*, 2013, **113**, 119–191.

66 H. Wang, H. Su, N. Wang, J. Wang, J. Zhang, J. H. Wang and W. Zhao, Recent development of reactional small-molecule fluorescent probes based on resorufin, *Dyes Pigm.*, 2021, **191**, 109351.

67 L. Tian, H. Feng, Z. Dai and R. Zhang, Resorufin-based responsive probes for fluorescence and colorimetric analysis, *J. Mater. Chem. B*, 2021, **9**, 53–79.